

Spin canted magnetism, decoupling of charge and spin ordering in NdNiO_3

Devendra Kumar* and K. P. Rajeev†

Department of Physics, Indian Institute of Technology Kanpur 208016, India

J. A. Alonso and M. J. Martínez-Lope

Instituto de Ciencia de Materiales de Madrid, CSIC, Cantoblanco, E-28049 Madrid, Spain

We report detailed magnetization measurements on the perovskite oxide NdNiO_3 . This system has a first order metal-insulator (M-I) transition at about 200 K which is associated with charge ordering. There is also a concurrent paramagnetic to antiferromagnetic spin ordering transition in the system. We show that the antiferromagnetic state of the nickel sublattice is spin canted. We also show that the concurrency of the charge ordering and spin ordering transitions is seen only while warming up the system from low temperature. The transitions are not concurrent while cooling the system through the M-I transition temperature. This is explained based on the fact that the charge ordering transition is first order while the spin ordering transition is continuous. In the magnetically ordered state the system exhibits ZFC-FC irreversibility, as well as history-dependent magnetization and aging. Our analysis rules out the possibility of spin-glass or superparamagnetism and suggests that the irreversibility arises from magnetocrystalline anisotropy and domain wall pinning.

PACS numbers: 75.60.-d, 75.60.Ej, 71.30.+h

Keywords: Nickelates, magnetic ordering, magnetization, hysteresis, magnetocrystalline anisotropy

I. INTRODUCTION

The rare earth nickelates (RNiO_3 , $\text{R} \neq \text{La}$) have been under active investigation for the past two decades because of the interesting electronic and magnetic properties exhibited by these systems.^{1,2} These oxides undergo a bandwidth controlled metal-insulator (MI) transition on changing the temperature, chemical or hydrostatic pressure.³⁻⁷ In the metallic state the structure of these nickelates is that of an orthorhombic distorted perovskite with space group $Pbnm$.⁸ The metal to insulator transition occurs with a structural transition which consists of an increase in the unit cell volume, a decrease in Ni-O-Ni bond angle and a symmetry lowering from orthorhombic $Pbnm$ to monoclinic $P2_1/n$. The symmetry lowering is understood in terms of charge ordering with a charge disproportionation $2\text{Ni}^{3+} \rightarrow \text{Ni}^{3+\delta} + \text{Ni}^{3-\delta}$ with $\delta \approx 0.2 - 0.3$.⁹⁻¹⁴ In the early reports, the M-I transition of these compounds was attributed to the opening of an Ni-O charge transfer gap created by band narrowing.³ But the occurrence of charge ordering at the M-I transition and some recent theoretical calculations suggest that the M-I transition owes its origin to the opening of a gap between the spin up e_g band of $\text{Ni}^{3-\delta}$ and the hardly spin polarized e_g band of $\text{Ni}^{3+\delta}$.¹⁵ In these compounds the higher temperature phase is metallic and the lower temperature phase is insulating. The M-I transition is of first order and is associated with a large thermal hysteresis and time dependent effects in transport properties such as resistivity and thermopower.¹⁶⁻¹⁹ During the cooling process, in the temperature window where hysteresis is seen, these compounds phase separate into insulating and supercooled metallic regions. The supercooled regions are metastable and they switch over to the insulating state stochastically giving rise to time dependence and hysteresis in transport properties.¹⁷⁻¹⁹

The nickelates also undergo a temperature driven magnetic transition, which is relatively less studied, because the higher magnetic moment of rare earth ion (e.g. Nd^{3+} moment $\approx 3.6\mu_B$) makes it difficult to get any information about the magnetic ordering of the Ni sublattice (Ni^{3+} moment $\approx 1\mu_B$) through magnetization measurements.^{1,20,21} Muon spin rotation experiments of Torrance et al. show that these compounds undergo a magnetic ordering from paramagnetic to an antiferromagnetic state on lowering the temperature.³ The magnetic ordering temperature (T_N) coincides with the M-I transition temperature (T_{MI}) for PrNiO_3 and NdNiO_3 , while it is lower than T_{MI} for all the other nickelates. The magnetic transition is of second order for all nickelates having $T_{\text{MI}} > T_N$,^{22,23} but for NdNiO_3 and PrNiO_3 where $T_{\text{MI}} = T_N$, the nature of the magnetic transition is difficult to probe independently. While one would expect the magnetic transition to be continuous as seen in other members of the series we note that there is at least one report which goes against this expectation and claim that the said transition is of first order.²³

Neutron diffraction experiments show that, below T_N , the magnetic arrangement of Ni moments is characterized by the propagation vector $(\frac{1}{2}, 0, \frac{1}{2})$ which suggests three possible magnetic structures, of which, two are collinear and one is non-collinear.^{9,24,25,27,28} The collinear magnetic structure consists of up-up down-down stacking of Ni magnetic moments, where each Ni moment is antiferromagnetically coupled to three of its nearest neighbors and ferromagnetically to the remaining three nearest neighbours. This magnetic structure implies that the orbital degeneracy of Ni^{3+} e_g^1 electrons should be lifted by an orbital ordering, a prediction which has not gathered any experimental support so far.²⁵ Soft X-ray resonant scattering experiments at the Ni $L_{2,3}$ edges show that the $(\frac{1}{2}, 0, \frac{1}{2})$ reflections are purely of magnetic origin with

no orbital contribution whatsoever thus more or less ruling out collinear magnetic order in the system.²⁹ In fact, the orbital degeneracy of the $\text{Ni}^{3+} e_g^1$ electron is found to be lifted by charge-ordering¹⁵ and this supports the existence of a non-collinear magnetic structure which does not require orbital ordering. The low temperature specific heat data and the resonant soft X-ray diffraction data of induced Nd magnetic moment in NdNiO_3 indicate that, in all likelihood, the ordering of Ni moments in NdNiO_3 is non-collinear.^{30,31}

In this work, for the first time, we report the magnetization of the Ni *sublattice*, which we extracted after carefully subtracting the contribution of the Nd moments from the total magnetization. The magnetization of the Ni sublattice shows weak ferromagnetism which indicates that the magnetic arrangement of the Ni moments is perhaps canted. The existence of weak ferromagnetism cannot be understood in terms of the magnetic structures referred to in the previous paragraph, even the noncollinear ones. This suggests that those magnetic structures do not represent the true picture and the actual magnetic arrangement of Ni moments could be quite different from what has been thought of so far. Further, we found that the supercooled metallic phase is magnetically ordered which indicates that the transition, on cooling, from the paramagnetic to the antiferromagnetic state happens at the nominal transition temperature (≈ 200 K) unlike the metal-insulator transition which is broadened and happens at lower temperatures as the supercooled metallic regions switch to the insulating phase stochastically. This shows that the connection between the magnetic transition and the metal-insulator transition is rather weak and they do decouple if the system is supercooled. Also, the magnetization of the Ni sublattice shows features such as FC-ZFC irreversibility which is indicative of the presence of frustration in the weak ferromagnetic state.

II. EXPERIMENTAL DETAILS

High quality polycrystalline NdNiO_3 pellets were prepared by a liquid mixture technique described elsewhere.³²

All the magnetic measurements were performed in a SQUID magnetometer (Quantum Design, MPMS XL). Since, in this work, we are trying to extract the small signal from the Ni moments buried under the much larger signal from the Nd moments it is a sine qua non that we are absolutely sure about the quality of the data. The magnetic signal from the samples of NdNiO_3 and NdGaO_3 , each of mass about 120mg, is 0.00262 emu and 0.00159 emu respectively at 150 K and 500 G. These numbers are more than three orders of magnitude higher than the level where artifacts start distorting the measured data.³³ Further, the sample holders used in SQUID measurements can give rise to misleading results when the background signal from the sample holder becomes large enough so that it can no longer be ignored compared

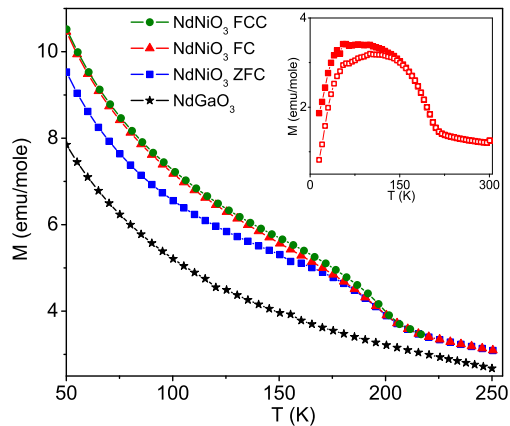


Figure 1: (Color Online) The temperature variation of the magnetization of NdNiO_3 in FCC (circles), FC (triangles), and in ZFC (squares) protocols at 500 Oe. The stars show the magnetization of NdGaO_3 at the same field. For NdGaO_3 the FCC, FC and ZFC magnetizations coincide. The inset shows the difference in magnetization of NdNiO_3 and NdGaO_3 down to 10 K at 1000 Oe in FC (upper curve, filled squares) and ZFC (lower curve, open squares) protocol. We used 119 mg of NdNiO_3 and 118 mg of NdGaO_3 for these measurements.

to the signal from the sample.³⁴ In our case, the sample holder is a piece of straw which gives a temperature independent signal of about -4×10^{-6} emu at 500 G which is about 600 times smaller than the signal from the NdNiO_3 sample at 150 K. From the aforementioned we see that artifacts or extraneous contributions are negligible compared to the magnetic signal of NdNiO_3 , and thus, our SQUID data can be confidently used for the critical analysis we are setting out to do.

The field dependent resistivity measurements were performed in a home made cryostat placed between the pole pieces of a large electromagnet. More details on the resistivity measurements are available in one of our earlier publications.¹⁷

III. RESULTS AND DISCUSSION

1. Magnetization measurements

Figure 1 shows the magnetization of NdNiO_3 and NdGaO_3 in FC, ZFC and FCC protocols at 500 Oe. In the FC protocol we cool the sample in the presence of a specified field and then record the magnetization while slowly warming up the sample keeping the field fixed. In the ZFC protocol we cool the sample in zero field to the lowest temperature and then apply the specified field and record the magnetization while warming up. In FCC protocol the magnetization is recorded while cooling in the specified field. The magnetization plots of NdNiO_3 show a shoulder around 200 K attributable to the ordering of Ni moments. We see that below 200 K the magnetization

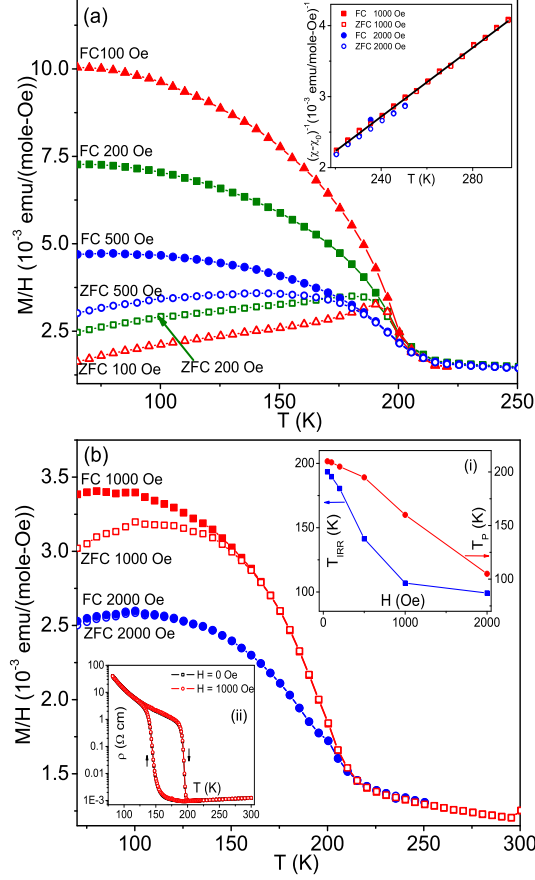


Figure 2: (Color Online) The dc magnetic susceptibility of the Ni sublattice versus temperature for FC and ZFC protocols at various fields. The inset of (a) shows that the susceptibility above 220 K follows the modified Curie-Weiss law shown in equation (1) quite closely. The top-right inset of (b) shows the temperature dependence of resistivity at zero field and 1000 Oe during cooling as well as warming. The bottom-left inset of (b) shows how T_{IRR} and T_P depend on the applied field. T_P is determined by Gaussian fitting of the ZFC curves close to their maxima.

of NdNiO₃ depends on the experimental protocol. The FCC magnetization is slightly higher than the FC magnetization while ZFC magnetization is lower than both FCC and FC magnetizations. Above 200 K, the FCC, FC, and ZFC curves overlap and are indistinguishable. The existence of thermal and magnetic history dependence in magnetization suggests that the system is not in thermodynamic equilibrium below 200 K. In contrast, for the reference sample NdGaO₃, the magnetization values in FCC, FC, and ZFC protocol coincide and follow the Curie law.

To extract the magnetization of Ni sublattice from the experimental data we subtract the contribution of Nd moments from that of NdNiO₃. The Nd magnetic

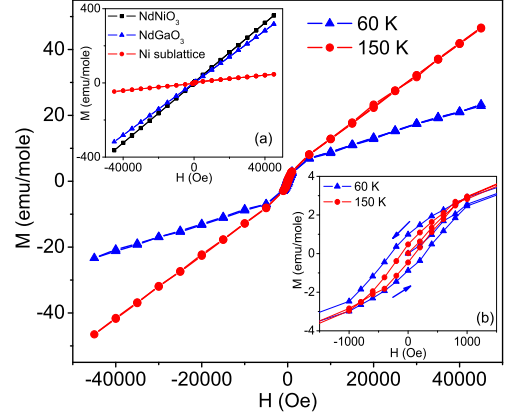


Figure 3: (Color Online) M-H curves for the Ni sublattice at 150 K and 60 K. The inset (a) displays the magnetization of NdNiO₃, NdGaO₃, and their difference at 150 K. The inset (b) shows an expanded view of the low field data of Ni sublattice.

Field (Oe)	C	θ	χ_0	χ^2/DOF	R^2
1000(FC)	0.043(4)	125(6)	0.00095(2)	1.314	0.99916
1000(ZFC)	0.043(4)	126(6)	0.00095(2)	1.271	0.99920

Table I: Fit parameters obtained from the fitting of equation (1) to the 1000 Oe magnetic susceptibility data of figure 2 above 220 K. The quality of the fit is clear from the fitted line to the red squares in the inset of fig 2(a) as well as from the low χ^2/DOF values and the R^2 values very close to unity presented in this table. For other field values the number of data points above 220 K and their span are not good enough to warrant comparable quality of fitting.

moment is estimated from the magnetization data of NdGaO₃ which has the same crystal structure and almost the same lattice parameters as NdNiO₃.¹⁹ Since gallium and oxygen ions have no magnetic moment, the magnetization of NdGaO₃ arises only from the contributions of the Nd moments sitting at the A sites of the perovskite structure. By subtracting the NdGaO₃ magnetization (per mole) from that of NdNiO₃ we should be able to calculate the magnetization of Ni sublattice, provided Nd moments behave in the same fashion in both NdGaO₃ and NdNiO₃. Unfortunately this method runs into rough weather because the Nd moments in NdNiO₃ tend to order at low temperature aided by the ordering of the Ni sublattice.

Neutron diffraction measurements on bulk NdNiO₃ show that the magnetic ordering of Nd moments starts below 40 K,^{25,26} while the synchrotron radiation data on thin films of NdNiO₃ suggest that magnetic ordering of Nd moments starts at T_{MI} but becomes significant only at low temperatures below 70 K.³¹ The higher Nd ordering temperature seen in the thin films may have a possible connection with the epitaxial strain in the films.³⁵ The ordering of Nd moments is thought to be induced by the direct exchange interaction with the neighboring Ni moments and is antiferromagnetic in nature while the

Nd moments in NdGaO₃ remain paramagnetic throughout the temperature range (See Ref. 31 and Fig. 1). So on cooling below the magnetic ordering temperature of Nd, the difference in the magnetization of NdNiO₃ and NdGaO₃ would drop drastically because the contribution of Nd moments to the magnetization of NdNiO₃ would fall due to their antiferromagnetic ordering. In our case, such a drastic drop in the difference in magnetization of NdNiO₃ and NdGaO₃ is seen to occur below about 50 K as is clear from the inset of Fig. 1. This suggests that the effect of Nd ordering becomes quite significant below 50 K, and sufficiently above this temperature, the magnetization of Ni sublattice could be obtained, to a reasonable degree of confidence, by the subtraction of NdGaO₃ magnetization from that of NdNiO₃.

2. Magnetic ordering of the Ni sublattice

In figure 2 we show the temperature dependence of ZFC and FC dc magnetic susceptibility of Ni sublattice between 100 Oe to 2000 Oe. Above 220 K, as is clear from the inset of figure 2(a), the data fit well to the modified Curie Weiss equation

$$\chi = C/(T - \theta) + \chi_0 \quad (1)$$

where C and θ are Curie and Weiss constants respectively, and χ_0 is a constant arising from Van Vleck and Pauli paramagnetism and Landau and core diamagnetism. The parameters obtained from the fitting of equation (1) to the 1000 Oe susceptibility data of figure 2, in the temperature range of 220-300 K, is shown in table I. The R^2 values very close to unity and the low χ^2/DOF values indicate that fit quality is very good.

The presence of possible defects in the crystalline lattice structure may also give a contribution to magnetic susceptibility, but that contribution is generally around 10^3 times smaller than our measured signal,^{36,37} and this fact allows us to ignore them.

The subtraction of NdGaO₃ magnetic susceptibility from that of NdNiO₃ cancels the temperature independent Van-Vleck and core contribution of Nd ions, and so χ_0 is free of these two. The core diamagnetic susceptibility of Ni ions is around -68×10^{-6} emu/mole³⁸ and the Landau diamagnetic susceptibility is connected to Pauli paramagnetic susceptibility by the equation $\chi^{Landau} = -(1/3)[m/m^*]^2 \chi^{Pauli}$, where m is the free electron mass and m^* is the effective mass of an electron in the conduction band. Since m^* is found to be significantly larger than m in this family of oxides,³⁹ the χ^{Landau} can be neglected in comparison to χ^{Pauli} .³⁸ Thus the χ_0 values shown in table I arise predominantly from the Pauli paramagnetism of itinerant electrons, and they are in good agreement with the values reported in Refs. 21 and 38. The Pauli paramagnetic susceptibility of NdNiO₃ is around two orders of magnitude larger than that calculated using the free-electron value which suggests that the electron correlation in these systems is very

strong.²¹ It is to be noted that we get a positive Weiss constant θ which is indicative of a ferromagnetic interaction in the magnetically ordered state. This is surprising considering the fact that neutron and resonant soft X-ray diffraction measurements show that the system has antiferromagnetic order below T_{MI} .^{9,24,25,27,28} In consonance with the above observation of a positive Weiss constant we point out that below 195 K, in FC measurements, the magnetic susceptibility increases on decreasing the temperature as would be expected in the case of ferrimagnets or canted antiferromagnets which behave as weak ferromagnets. See figure 2.

In figure 3 we have shown the field dependence of the magnetization of the Ni sublattice. The inset (a) of the figure shows the magnetization versus field for NdNiO₃, NdGaO₃ and the Ni sublattice at 150 K. The Ni sublattice magnetization is obtained by subtracting the contribution of Nd moments (obtained from NdGaO₃) from that of NdNiO₃. In the main panel of figure 3 and its inset (b) we show the magnetization versus field for the Ni sublattice at 150 K and 60 K. The M-H curves show a small hysteresis at small fields, while at higher fields, the M-H curves behave as that of a typical antiferromagnet, with M varying linearly with H , which leads to the conclusion that this system is a spin-canted antiferromagnet.⁴⁰ The presence of spin canted magnetism (weak ferromagnetism) cannot be explained on the basis of the magnetic structures proposed in the literature (Refs. 23, 24, 26). This is because the sum of the Ni magnetic moments in the proposed collinear as well as the non-collinear magnetic structure is zero (See figure 5 of Ref. 28). Thus our experimental data clearly show that the magnetic structures proposed in the literature are not the true magnetic picture of NdNiO₃. Further investigations are required to confirm this new experimental finding.

Referring to the inset (b) of figure 3, we see that, the coercivity (H_C) is temperature dependent below T_N , and it increases on lowering the temperature. Since coercivity is related to magnetic anisotropy, this suggests that the magnetic anisotropy increases on decreasing the temperature.

3. Magnetic state of the supercooled phase

The transport properties of NdNiO₃ show thermal hysteresis which is attributed to the presence of supercooled metallic regions below the transition temperature.¹⁷⁻¹⁹ Now the question we would like to ask is this: What is the magnetic state of the supercooled metallic regions? Are they paramagnetic or antiferromagnetic? In other words we are asking whether the paramagnetic to antiferromagnetic transition, when we cool the system through its magnetic transition temperature (200 K), takes place at that temperature or does it take place along with the M-I transition of the metastable phase at a lower temperature? In order to throw some light on this issue we mea-

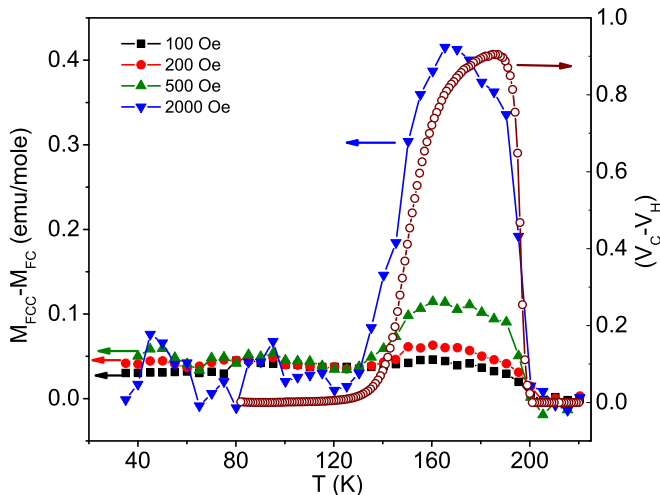


Figure 4: (Color Online) The temperature variation of the difference in magnetization, $M_{\text{FCC}} - M_{\text{FC}}$, of NdNiO_3 between cooling and heating runs at 100 Oe, 200 Oe, 500 Oe and 2000 Oe (solid symbols). The open circles show the difference in the metallic volume fraction, $V_{\text{C}} - V_{\text{H}}$, between cooling and heating runs.

sured the thermal hysteresis of magnetization. In figure 4 we show the difference in cooling and heating cycle magnetization, $M_{\text{FCC}} - M_{\text{FC}}$, of NdNiO_3 at a few field values in the range 100 Oe to 2000 Oe. The data show that between 200 K and 120 K, the magnetization of the cooling cycle is higher than that of the heating cycle. The difference in the magnetization is maximum around 170 K. Figure 4 also shows the difference in the metallic volume fractions between the cooling and heating runs $V_{\text{C}} - V_{\text{H}}$, taken from reference 17. The difference in the magnetizations and the difference in the metallic volume fractions have remarkably similar temperature dependence which suggests that they originate from a common underlying physical mechanism. In a cooling run, below T_{MI} , the system contains supercooled metallic and insulating regions, while in a heating run, it is mostly insulating.^{17–19} Therefore $V_{\text{C}} - V_{\text{H}}$ represents the volume fraction of supercooled metallic regions. So the correlation between the thermal hysteresis in magnetization and the supercooled metallic volume fraction indicates that the supercooled metallic regions have a higher magnetic moment compared to the insulating regions.

The Ni moments are paramagnetic in the normal metallic state ($T > T_{\text{MI}}$) while they show a spin-canted antiferromagnetic ordering in the insulating state. Also, the spin-canted insulating state has a higher susceptibility than the paramagnetic metallic state (see figure 2). This suggests that if the supercooled metallic regions were paramagnetic, as above T_{MI} , then the magnetization of NdNiO_3 in a cooling run, where below T_{MI} the system consists of supercooled metallic and insulating regions, should be lower than that in a heating run where the system is expected to be almost fully insulating. But the experimental results discussed in the pre-

vious paragraph contradict this which indicates that the supercooled metallic regions are not paramagnetic. To make things more concrete, we compare the observed difference in the magnetization of cooling and heating runs to the expected value of the difference if the supercooled regions were paramagnetic. In the cooling run, at 170 K, the volume fraction of the supercooled metallic regions is around 0.9 from figure 4. The dc magnetic susceptibility of the paramagnetic metallic phase at 2000 Oe (Figure 2), extrapolated down to 170 K, is about 20% smaller than that of the insulating phase which suggests that if the thermal hysteresis in the magnetization is because of paramagnetic ordering of supercooled metallic regions, then, according to our estimate, the difference in the magnetization of the cooling and heating runs should be around -0.9 emu/mole. But the observed difference in the magnetization is $+0.4$ emu/mole which has the wrong sign and is smaller in magnitude than the expected value. This observation strongly suggests that the supercooled metallic regions are antiferromagnetic with canted spins just like the insulating state. The small positive difference in magnetization between cooling and heating is proportional to the volume fraction of supercooled metallic regions and hence we conclude that this difference in susceptibility is temperature independent. This suggests that the observed difference in cooling and heating cycle magnetization is coming from itinerant electrons in the supercooled metallic state through Pauli paramagnetic and Landau diamagnetic contributions.⁴¹ Thus we see that the metallic state is paramagnetic above T_{MI} and on cooling below T_{MI} , while a fraction of the high temperature metallic phase exists in its supercooled state, the magnetic ordering of the whole sample switches to an antiferromagnetic state at T_{N} .

From the above discussion, we conclude that in NdNiO_3 , even though the charge ordering and magnetic ordering occur at the same temperature (in equilibrium) they are not strongly coupled and occur independently of each other. Incidentally, we note that except in PrNiO_3 and NdNiO_3 of the nickelate series, the two transitions occur at different temperatures which supports the conclusion that the two transitions are only weakly coupled. The antiferromagnetic order of the supercooled metallic regions rules out the presence of any metastable magnetic phase associated with the magnetic transition and suggests that the magnetic transition is continuous in nature. This result removes the ambiguity associated with the nature of the magnetic transition in nickelates where $T_{\text{MI}} = T_{\text{N}}$; the magnetic transition is continuous which is consistent with the other members of the series where $T_{\text{MI}} > T_{\text{N}}$.

4. The FC-ZFC irreversibility

The FC and ZFC magnetic susceptibilities show a history dependence with a bifurcation between the two curves at a temperature known as the temperature of

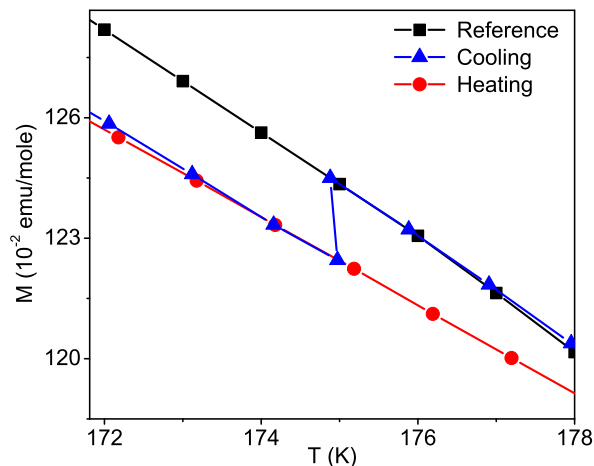


Figure 5: (Color Online) Memory experiment in the FC protocol with intermediate stops of one hour at 175, 150, 125 and 110 K. The field is switched off during each stop. The data close to 175 K is shown here. The black squares show the FC reference which is the magnetization in FCC protocol(after removing the contribution of thermal hysteresis).

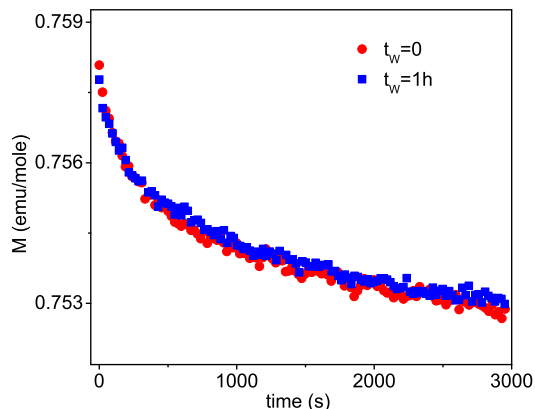


Figure 6: (Color Online) The time decay of thermoremanent magnetization of NdNiO₃ at 80 K (red circles). The blue squares show the decay of thermoremanent magnetization with a one hour wait time.

irreversibility (T_{IRR}). See inset (i) figure 2(b). The temperature of irreversibility depends on the magnetic field and it decreases on increasing the magnetic field. For fields greater than 2 kOe the FC and ZFC curves superpose. Behavior such as this where the magnetic susceptibility depends on measurement history has been observed in non-equilibrium systems such as spin-glasses,^{42–44} superparamagnets,⁴⁵ cluster-glasses,^{46,47} supercooled systems,^{48,49} and also in anisotropic ferromagnets and ferrimagnets.^{50–54} The ZFC data show a peak, and the peak broadens and shifts to low temperatures on increasing the magnetic field. We analysed the nature of this peak and found that the peak temperature (T_P) as a function of field (H) does not behave as in the case of spin-glasses, cluster-glasses,⁵⁵ or superparamagnets^{56,57} which indicates that the system is neither a spin-glass

nor a superparamagnet. We also rule out supercooling as a possible reason for the FC-ZFC irreversibility by the following argument. The resistivity measurements show a thermal history dependence which is attributed to the presence of supercooled metallic regions below T_{MI} . We did not observe any significant magnetic field or magnetic history dependence in transport properties which suggests that the volume fraction of supercooled metallic regions is not altered by the application of a magnetic field. See inset (ii) of figure 2(b). The lack of dependence of resistivity on applied magnetic field has also been reported earlier by Mallik et al.⁵⁸ From these results, we infer that the magnetic history dependence of the dc magnetic susceptibility (see figure 2(a) and (b)) cannot be originating from the supercooled metallic phases. So far our analysis has shown that the magnetic hysteresis does not arise from spin-glass or cluster-glass nature, superparamagnetism or supercooling. This leaves us with the only possibility that the magnetic hysteresis in this system is arising from magnetic anisotropy of the spin canted magnetic domains.

To be doubly sure that the history dependent FC and ZFC susceptibility of the Ni sublattice has nothing to do with superparamagnetism or spinglass nature, we performed FC, ZFC memory and aging experiments. Since the Nd moments are paramagnetic, they would not have any role in the memory and aging of NdNiO₃. Thus if any such effect is seen in this system it would have to be attributed to the Ni sublattice. The FC memory experiments were performed with intermediate stops of one hour at 175, 150, 125, and 100 K. In these experiments the system is cooled in a 100 Oe field from 220 K to 80 K and then heated back to 180 K to remove the influence of supercooled metastable regions on dynamic behavior. Subsequently the system is cooled from 180 K to 80 K with intermediate stops of 1 hour at 175, 150, 125, and 100 K. The field was switched off during the intermediate stops. The magnetization is recorded while cooling and then during the subsequent heating. The FC memory data at 175 K is shown in figure 5. We can see that immediately after an intermediate stop the magnetization does not go back to its pre-stop value after switching on the field. In the subsequent heating run, we did not find any memory of the intermediate stops and this rules out the possibility of superparamagnetism or spin-glass behavior in the system.⁴⁴ We also carried out ZFC memory experiments on the system at 170 K and the result was negative. This confirms the conclusions we arrived at from the FC memory experiments and once again rules out a spin-glass state.⁴⁴

In figure 6 we show the results of the FC ageing experiment. In this experiment one essentially measures the time decay of thermoremanent magnetization along with wait time dependence. To begin with we cool the system from 250 K to 80 K in the presence of 100 Oe field, wait for the duration t_w at 80 K with the field on, and then switch off the field and record the magnetization as a function of time. It is clear from the figure that the sys-

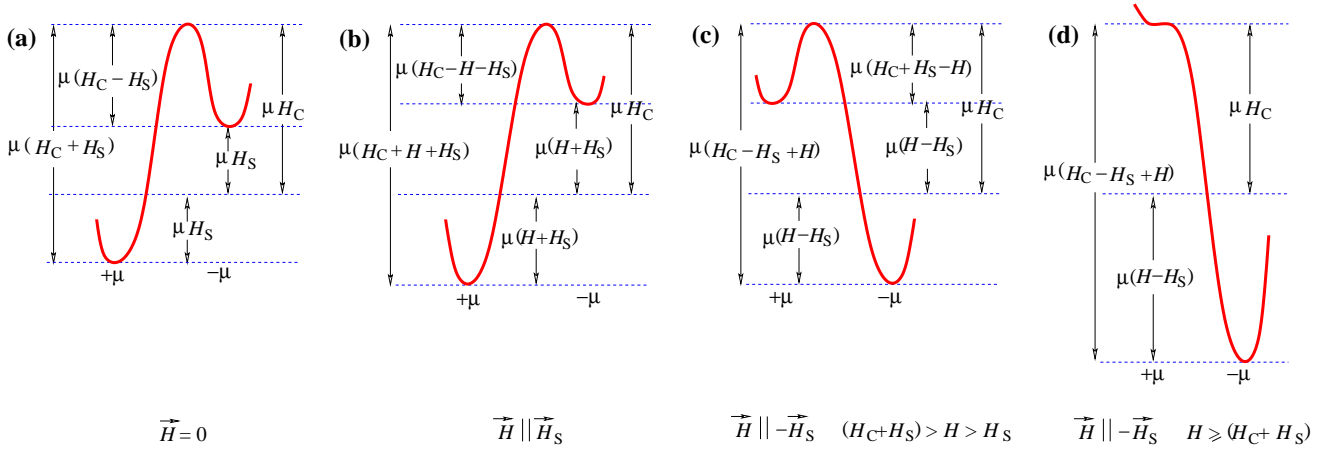


Figure 7: (Color Online) The free energy profile of a bistable subsystem at various applied fields

tem does not show any noticeable wait time dependence in FC ageing and this yet again rules out the possibility of the system being a spin glass or a superparamagnet.⁴⁴

The irreversibility of the FC and ZFC magnetic susceptibility in a system which is neither a spin-glass nor superparamagnetic can be understood in terms of a competition between the magnetocrystalline anisotropy and domain wall pinning on the one hand and applied field and thermal energy on the other.^{50–54} Below the temperature of magnetic ordering, a magnetically ordered material consists of uniformly magnetized regions which are known as magnetic domains. At any temperature T and applied field H , the free energy of the magnetic systems have a number of local minima which are determined by the arrangement of the domains inside the magnetic material. These local minima states are separated by energy barriers which arise due to magnetocrystalline anisotropy and domain wall pinning. When the thermal energy is greater than the energy barrier of the metastable state in which the system is trapped, the system can explore the neighboring states in search of the global minimum or the equilibrium state. The free energy configuration is a function of applied magnetic field H and temperature T and on changing H or T (which changes the magnetocrystalline anisotropy) the system evolves from one configuration to another.⁵⁹ We shall make an attempt to understand our system on the basis of the Preisach model in which the free energy configuration is decomposed into an ensemble of bistable subsystems.⁵⁹ A bistable subsystem consists of two metastable states separated by an energy barrier. The two states have moments oriented in opposite directions and are termed as $\pm\mu$ states. The free energy of these states in the absence of applied magnetic field is determined by the local interaction field (H_S) and the the coercive field (H_C). H_S is the net magnetic field produced at the location of the moment μ by the magnetic moments of all the neighboring domains. If $H_S = 0$ then μH_C represents the anisotropy energy barrier that has to be crossed to go from $+\mu$ to $-\mu$ state or vice versa. The barrier height seen from the $+\mu$ side is $\mu(H_C + H_S)$

while from the $-\mu$ side it is $\mu(H_C - H_S)$. See figure 7 (a). The application of a magnetic field (H) changes the free energy of the metastable states which in turn affects the effective height of the energy barrier. We also note that a change in the temperature can also affect the free energy barrier through its effect on magnetocrystalline anisotropy.^{53,54,59}

In the following paragraphs we discuss qualitatively the FC-ZFC irreversibility and the remanent magnetization using the standard Preisach model. Thereafter we apply it to understand the observed results of aging experiments.

In ZFC protocol when the system is cooled below T_N each subsystem will be in its lower energy state which is determined by H_S (Figure 7 (a)). On applying a magnetic field, depending on the direction and strength of the applied field, the low energy state of the subsystem may remain as the low energy state (Figure 7 (b)), or may become metastable or unstable (Figure 7 (c) and (d)). If $\vec{H} \parallel -\vec{H}_S$, the subsystems for which H is larger than $H_C + H_S$, will flip to their new low energy state (Figure 7 (d)). It is this flipping that gives rise to the initial value of the ZFC magnetization of the system. The subsystems for which H is less than $(H_C + H_S)$, are now in a metastable state (Figure 7 (c)). These subsystems will undergo a thermally activated transformation, which gives rise to a slowly rising time dependent ZFC magnetization even if the magnetic field is held fixed. On increasing the temperature, H_C decreases and because of this more number of subsystems will flip to their new low energy state and this increases the ZFC magnetization further. As one increases the temperature the ZFC magnetization curve will attain a peak when the most probable H_C value of the Barkhausen moment (μ) becomes equal to the applied field H .

In the FC protocol the subsystems get trapped in their low energy states, as the sample is cooled through the magnetic ordering temperature in the presence of an applied field. At a constant field, a decrease in temperature increases the energy barrier (because of increase in H_C),

but this does not affect the relative positions of the $+\mu$ and $-\mu$ states. Thus in the FC protocol there is hardly any change of state of the bistable subsystems when cooling through T_N . The temperature dependence observed in the FC magnetization is because of temperature dependence of the Barkhausen moment $\mu(T)$. That is why the shape of an FC magnetization curve is nearly the same for all fields.

If we switch off the applied field in the FC protocol, the subsystems for which applied field \vec{H} is opposite and greater in magnitude than \vec{H}_S will result in their low energy state becoming a high energy state and vice versa. This can be understood looking at figure 7 where the initial states shown in figures 7 (c) or (d) switch to the final state shown in figure 7 (a) on removal of the applied field. Of these subsystems, those which have $H_S \geq H_C$, will become unstable on removing the field, and their change of state constitutes the initial loss of FC magnetization. The other subsystems (which have $H_S < H_C$) will become metastable and their thermally activated transformation from a metastable to a new lower energy state gives a further slow decay in FC magnetization.

At this point let us examine the effect of aging (wait time dependence) on the system. All the subsystems occupy their lower energy state on cooling through T_N . Thus, after cooling, if we wait for a few hours before switching off (or on) the field, it will not affect the population of the $\pm\mu$ states and hence we would not get any effect of aging on magnetic relaxation.

IV. CONCLUSION

We performed detailed magnetization measurements on NdNiO_3 and extracted the magnetization of Ni sub-

lattice after removing the contribution of the rare earth Nd ion. Our results indicate the presence of weak ferromagnetism coexisting with antiferromagnetic order in the Ni sublattice. We argued that the weak ferromagnetism is due to canting of antiferromagnetic spins. Further we found that in contrast to the normal metallic state, the supercooled metallic regions are magnetically ordered. This shows that while cooling the metal insulator transition occurs over a temperature range of 200 K to 110 K, the magnetic ordering is sharp and occurs at 200 K. The absence of metastable phases in the magnetic transition suggests that the magnetic transition is continuous similar to other members of the series that have $T_{MI} > T_N$. Below T_N , the ZFC-FC magnetizations diverge exhibiting irreversibilities, that could remind one of a spin-glass state. However, our analysis shows that the system is neither a spin-glass nor a superparamagnet, and the irreversibilities arise from the temperature-dependent magnetocrystalline anisotropy and domain-wall pinning.

V. ACKNOWLEDGEMENTS

DK thanks the University Grants Commission of India for financial support. JAA and MJM-L acknowledge the Spanish Ministry of Education for funding the Project MAT2010-16404.

* Electronic address: deveniit@gmail.com; Present Address: UGC-DAE Consortium for Scientific Research, University Campus, Khandwa Road, Indore-452001, India.

† Electronic address: kpraj@iitk.ac.in

¹ M. L. Medarde, J. Phys.: Condens. Matter **9**, 1679 (1997).

² G. Catalan, Phase Transitions **81**, 729 (2008).

³ J. B. Torrance, P. Lacorre, A. I. Nazzal, E. J. Ansaldo, and Ch. Niedermayer, Phys. Rev. B **45**, 8209 (1992).

⁴ X. Obradors, L. M. Paulius, M. B. Maple, J. B. Torrance, A. I. Nazzal, J. Fontcuberta, and X. Granados, Phys. Rev. B **47**, 12353 (1993).

⁵ P. C. Canfield, J. D. Thompson, S. W. Cheong, and L. W. Rupp, Phys. Rev. B **47**, 12357 (1993).

⁶ J.-S. Zhou, J. B. Goodenough, and B. Dabrowski, Phys. Rev. Lett. **94**, 226602 (2005).

⁷ A. Tiwari, C. Jin, and J. Narayan, Appl. Phys. Lett. **80**, 4039 (2002).

⁸ P. Lacorre, J. B. Torrance, J. Pannetier, A. I. Nazzal, P. W. Wang, and T. C. Huang, J. Solid State Chem. **91**, 225 (1991).

⁹ J. A. Alonso, J. L. García-Munõz, M. T. Fernández-Díaz,

M. A. G. Aranda, M. J. Martínez- Lope, and M. T. Casais, Phys. Rev. Lett. **82**, 3871 (1999).

¹⁰ J. A. Alonso, M. J. Martínez- Lope, M. T. Casais, J. L. García-Munõz, and M. T. Fernández-Díaz, Phys. Rev. B **61**, 1756 (2000).

¹¹ J. A. Alonso, J. L. García-Munõz, M. T. Fernández-Díaz, M. A. G. Aranda, M. J. Martínez- Lope, and M. T. Casais, Phys. Rev. B **64**, 094102 (2001).

¹² U. Staub, G. I. Meijer, F. Fauth, R. Allenspach, J. G. Bednorz, J. Karpinski, S. M. Kazakov, L. Paolasini, and F. d'Acapito, Phys. Rev. Lett. **88**, 126402 (2002).

¹³ M. Medarde, M. T. Fernández-Díaz, and Ph. Lacorre, Phys. Rev. B **78**, 212101 (2008).

¹⁴ J. L. García-Munõz, M. A. G. Aranda, J. A. Alonso, and M. J. Martínez- Lope, Phys. Rev. B **79**, 134432 (2009).

¹⁵ I. I. Mazin, D. I. Khomskii, R. Lengsdorf, J. A. Alonso, W. G. Marshall, R. M. Ibberson, A. Podlesnyak, M. J. M. J. Martínez- Lope, and M. M. Abd-Elmeguid, Phys. Rev. Lett. **98**, 176406 (2007).

¹⁶ X. Granados, J. Fontcuberta, X. Obradors, and J. B. Torrance, Phys. Rev. B **46**, 15683 (1992).

- ¹⁷ D. Kumar, K. P. Rajeev, J. A. Alonso, and M. J. Martínez-Lope, *J. Phys: Condensed Matter* **21**, 185402 (2009).
- ¹⁸ D. Kumar, K. P. Rajeev, J. A. Alonso, and M. J. Martínez-Lope, *J. Phys: Condensed Matter* **21**, 485402 (2009).
- ¹⁹ D. Kumar, K. P. Rajeev, A. K. Kushwaha, and R. C. Budhani, *J. Appl. Phys.* **108**, 063503 (2010).
- ²⁰ J. Blasco, M. Castro, and J. García, *J. Phys: Condensed Matter* **6**, 5875 (1994).
- ²¹ J. Pérez, J. Stankiewicz, J. Blasco, M. Castro, and J. García, *J. Phys: Condensed Matter* **8**, 10393 (1996).
- ²² J. Pérez-Cacho, J. Blasco, J. García, M. Castro, and J. Stankiewicz, *J. Phys: Condensed Matter* **11**, 405 (1999).
- ²³ A. Caytuero, H. Micklitz, F. J. Litterst, and E. M. Baggio-Saitovitch, *Phys. Rev. B* **74**, 094433 (2006).
- ²⁴ J. L. García-Munõz, J. Rodríguez-Carvajal, and P. Lacorre, *Europhys. Lett.* **20**, 241 (1992).
- ²⁵ J. L. García-Munõz, J. Rodríguez-Carvajal, and P. Lacorre, *Phys. Rev. B* **50**, 978 (1994).
- ²⁶ J. L. García-Munõz, P. Lacorre, and R. Cywinski, *Phys. Rev. B* **51**, 15197 (1995).
- ²⁷ M. T. Fernández-Díaz, J. A. Alonso, M. J. Martínez-Lope, M. T. Casais, and J. L. García-Munõz, *Phys. Rev. B* **64**, 144417 (2001).
- ²⁸ G. Giovannetti, S. Kumar, D. Khomskii, S. Picozzi, and J. van den Brink, *Phys. Rev. Lett.* **103**, 156401 (2009).
- ²⁹ V. Scagnoli, U. Staub, A. M. Mulders, M. Janousch, G. I. Meijer, G. Hammerl, J. M. Tonnerre, and N. Stojic, *Phys. Rev. B* **73**, 100409 (2006).
- ³⁰ F. Bartolomé, J. Bartolomé, and R. S. Eccleston, *J. Appl. Phys.* **87**, 7052 (2000).
- ³¹ V. Scagnoli, U. Staub, Y. Bodenthin, M. García-Fernández, A. M. Mulders, G. I. Meijer, and G. Hammerl, *Phys. Rev. B* **77**, 115138 (2008).
- ³² N. E. Massa, J. A. Alonso, M. J. Martínez-Lope, I. Rasines, *Phys. Rev. B* **56**, 986 (1997).
- ³³ A. Ney, T. Kammermeier, V. Ney, K. Ollefs, and S. Ye, *J. Magn. Magn. Mater* **320**, 3341 (2008).
- ³⁴ N. Casañ-Pastor, P. GómezRomero, and L. C.W. Baker, *J. Appl. Phys.* **69**, 5088 (1991).
- ³⁵ A. Baena, L. Brey, and M. J. Calderón, *Phys. Rev. B* **83**, 064424 (2011).
- ³⁶ R. R. Nair, M. Sepioni, I-Ling Tsai, O. Lehtinen, J. Keinonen, A. V. Krashenninnikov, T. Thomson, A. K. Geim, and I. V. Grigorieva, *Nature Physics* **8**, 199 (2012).
- ³⁷ H. J. Bornemann, W. Walukiewicz, and D. E. Bliss, *Phys. Rev. B* **46**, 9849 (1992).
- ³⁸ X. Q. Xu, J. L. Peng, Z. Y. Li, H. L. Ju, and R. L. Greene, *Phys. Rev. B* **48**, 1112 (1993).
- ³⁹ K. P. Rajeev, G. V. Shivashankar and A. K. Raychaudhuri, *Solid State Commun.* **79**, 591 (1991).
- ⁴⁰ S. Chikazumi, *Physics of Ferromagnetism* (Oxford University Press 1997) Chapter 7, page 151.
- ⁴¹ The χ_0 term in Table 1 represents the contribution of temperature independent susceptibilities (which includes Pauli & Van Vleck paramagnetism and Landau & core diamagnetism). Now the difference $M_{FCC} - M_{FC}$ at 170 K is 0.4 emu/mole for 2000 Oe (Figure 4). Converted to susceptibility the difference turns out to be around 0.0002 emu/mole-Oe. In Table 1, the χ_0 value is around 0.00095 emu/mole-Oe, and after removing the core diamagnetism, the Pauli and Landau contribution comes around 0.0009 emu/mole-Oe which is of the same order as the difference in susceptibility.
- ⁴² J. A. Mydosh, *Spin Glasses: An Experimental Introduction* (Taylor and Francis London 1993).
- ⁴³ S. D. Tiwari and K. P. Rajeev, *Phys. Rev. B* **72**, 104433 (2005).
- ⁴⁴ V. Bisht and K. P. Rajeev, *J. Phys. : Condens. Matter* **22**, 016003 (2010).
- ⁴⁵ M. Knobel, W. C. Nunes, L. M. Socolovsky, E. De Biasi, J. M. Vargas, and J. C. Denardin, *J. Nanosci. Nanotechnol.* **8**, 2836 (2008).
- ⁴⁶ I. G. Deac, J. F. Mitchell, and P. Schiffer, *Phys. Rev. B* **63**, 172408 (2001).
- ⁴⁷ X. H. Huang, J. F. Ding, Z. L. Jiang, Y. W. Yin, Q. X. Yu, and X. G. Lia, *J. Appl. Phys.* **106**, 083904 (2009).
- ⁴⁸ P. Chaddah, K. Kumar, and A. Banerjee, *Phys. Rev. B* **77**, 100402(R) (2008).
- ⁴⁹ M. K. Chattopadhyay, S. B. Roy, and P. Chaddah, *Phys. Rev. B* **72**, 180401 (2005).
- ⁵⁰ P S Anil Kumar, P A Joy, and S K Date, *J. Phys. : Condens. Matter* **10**, L487 (1998).
- ⁵¹ P S Anil Kumar, P A Joy, and S K Date, *Bull. Mater. Sci.* **23**, 97 (2000).
- ⁵² P A Joy, P S Anil Kumar, and S K Date, *J. Phys. : Condens. Matter* **10**, 11049 (1998).
- ⁵³ T. Song, R. M. Roshko, and E. D. Dahlberg, *J. Phys. : Condens. Matter* **13**, 3443 (2001).
- ⁵⁴ R.M. Roshko and L. Xi, *J. Appl. Phys.* **93**, 6653 (2003).
- ⁵⁵ R.L. de Almeida and D.J. Thouless, *J. Phys. A* **11**, 983 (1978).
- ⁵⁶ R.K. Zheng, Hongwei Gu, Bing Xu, X.X. Zhang, *J. Phys. : Condens. Matter* **18**, 5905 (2006).
- ⁵⁷ V. Bisht, K.P. Rajeev, S. Banerjee, *Solid State Communications* **150**, 884 (2010).
- ⁵⁸ R. Mallik, E V Sampathkumaran, J A Alonso, and M. J. Martínez-Lope, *J. Phys: Condensed Matter* **10**, 3969 (1998).
- ⁵⁹ G. Bertotti, *Hysteresis in Magnetism* (Academic Press 1993).